Short Papers

Fingerprint Indexing Based on Novel Features of Minutiae Triplets

Bir Bhanu, *Fellow*, *IEEE*, and
Xuejun Tan, *Student Member*, *IEEE*

Abstract—This paper is concerned with accurate and efficient indexing of fingerprint images. We present a model-based approach, which efficiently retrieves correct hypotheses using novel features of triangles formed by the triplets of minutiae as the basic representation unit. The triangle features that we use are its angles, handedness, type, direction, and maximum side. Geometric constraints based on other characteristics of minutiae are used to eliminate false correspondences. Experimental results on live-scan fingerprint images of varying quality and NIST special database 4 (NIST-4) show that our indexing approach efficiently narrows down the number of candidate hypotheses in the presence of translation, rotation, scale, shear, occlusion, and clutter. We also perform scientific experiments to compare the performance of our approach with another prominent indexing approach and show that the performance of our approach is better for both the live scan database and the ink based database NIST-4.

Index Terms—Fingerprint identification, indexing performance, *NIST-4* database, triangle features.

1 Introduction

FINGERPRINTS have long been used for person recognition due to their uniqueness and immutability. There are two general ways in which fingerprint based biometric systems are used: verification and identification. In verification, the user inputs a fingerprint image and claims an identity (ID), the system then verifies whether the input image is consistent with the input ID. In identification, which is more complex than verification, the user only inputs a fingerprint image, the system identifies potential corresponding fingerprints in the database. Efficient identification of fingerprints is still a challenging problem, since the size of the fingerprint image database can be large and there can be significant distortions between different impressions of the same finger. These distortions include: 1) translation, rotation, and scale because of different positions and downward pressure of the finger, 2) shear transformation as the finger may exert a different shear force on the surface, and 3) occlusion and clutter because of scars, dryness, sweat, smudge, etc. The problem of identifying a fingerprint can be stated as: Given a fingerprint database and a query fingerprint, obtained in the presence of translation, rotation, scale, shear, occlusion, and clutter, does the query fingerprint resemble any of the fingerprints in the database?

2 Related Research and Our Contributions

2.1 Related Research

There are three kinds of approaches to solve the fingerprint identification problem: 1) repeat the verification procedure for each fingerprint in the database, 2) fingerprint classification, and 3) fingerprint indexing. If the size of the database is large, the first approach is impractical. Although the scheme adopted by the FBI defines eight classes, generally, classification techniques [3], [6], [11] attempt to classify fingerprints into five classes: Right Loop (R), Left Loop (L), Whorl (W), Arch (A), and Tented Arch (T). However, the problem with classification technique is that the number of principal classes is small and the fingerprints are unevenly distributed (31.7 percent, 33.8 percent, 27.9 percent, 3.7 percent, and 2.9 percent for classes R, L, W, A, and T). The classification approach does not narrow down the search enough in the database for efficient identification of a fingerprint. The goal of the third approach, called indexing, is to significantly reduce the number of candidate hypotheses to be considered by the verification algorithm. Thus, an indexing technique can be considered as front-end processing, which would then be followed by back-end verification processing in a complete fingerprint recognition system. For multidimensional indexing methods, readers are referred to a survey article by Gaede and Gunther [14].

A prominent approach for fingerprint indexing is by Germain et al. [4]. They use the triplets of minutiae in their indexing procedure. The features they use are: the length of each side, the ridge count between each pair of vertices, and the angles that the ridges make with respect to the X-axis of the reference frame. The problems with their approach are:

1. the length changes are not insignificant under shear and other distortions,
2. ridge counts are very sensitive to image quality,
3. the angles change greatly with different quality images of the same finger, and
4. uncertainty of minutiae locations is not modeled explicitly.

As a result, bins that are used to quantize the "invariants" have to be large, which increases the probability of collisions and causes the performance of their approach to degrade. Our technique follows their work in that we also use the triplets of minutiae. However, the features that we use are quite different from theirs. The features that we use are: triangle's angles, handedness, type, direction, and maximum side. These features are different, new, and more robust than the features used by Germain et al. Table 1 shows the substantive differences between these two approaches. Their approach is basically an indexing method where the top hypothesis is taken as the identification result as has been done by several researchers (e.g, Jones and Bhanu [13])

2.2 Contributions of this Paper

1. An indexing algorithm, based on novel features formed by the triplets of minutiae and associated performance analysis are presented on two different data sets.
2. The indexing performance is demonstrated in a principled manner by using triplets as the basic representation unit.
3. Unlike the previously published research (see Table 2), where ad hoc personalized criteria, partial data, or handcrafted preprocessing are used for the selection of images to demonstrate the results, in this paper the *entire NIST-4* database is processed and analyzed in an automated manner in a black-box approach.[1]
4. Comparisons of the performance of our approach with Germain et al.'s approach are carried out, which show that our approach has performed better for both the live scan database and the ink based database *NIST-4*.

3 Technical Approach

Our system for fingerprint identification is composed of two stages: an offline stage and an online stage. The model database and indexing structure are constructed during the offline stage,

• *The authors are with the Center for Research in Intelligent Systems, University of California, Riverside, Riverside, CA 92521.*
E-mail: {bhanu, xtan}@cris.ucr.edu.

Manuscript received 23 Feb. 2001; revised 22 Apr. 2002; accepted 16 Oct. 2002. Recommended for acceptance by A. Khotanzad.
For information on obtaining reprints of this article, please send e-mail to: tpami@computer.org, and reference IEEECS Log Number 113674.

1. *Black-box* approach means no specific data tuning within the black-box, where the algorithm processes the entire input image.

TABLE 1
Comparison between Germain et al.'s [4] Approach and Bhanu and Tan's Approaches

Characteristics of the approach	Germain et al.'s approach	Bhanu & Tan's approach – this paper	Comments
Indexing components	Length of each side	Maximum length of three sides	Max. side is less sensitive to shear
	Three angles at triangle's vertices that ridges make with respect to the X-axis of the reference frame (local orientation)	Median and minimum angles of the triangles formed by the triplets of minutiae	Our angles are invariant to translation, rotation, and scale, and robust to shear. The errors in estimating local orientation angles in Germain et al.'s approach could be significant
	Ridge counts between every two vertices of a triangle	Triangle's handedness, type, and direction	Ridge count is sensitive to image quality
Indexing scheme	Flash	Hashing	
Geometric constraints	None	Yes	Constraints limit the size of the search space in our approach
Equivalent scale, bin size and data distortion	No explicit model, quantization for three sides is used	Only maximum side is affected by quantization	Germain et al. can not effectively deal with significant distortion by quantization alone
Shear	No explicit model, quantization is used	Threshold for angles	Shear not only affects side length, but also local orientation (see above)
Image database size	97492	1000 (our database) and 4000 (*NIST-4* [9])	Germain et al.'s database is propriety, *NIST-4* is public
# of test images	657 (<1% of database)	600 (100%) our database and 2000 (100%) *NIST-4*	Germain et al. do not use test images which are not in the database

TABLE 2
NIST-4 Database Used in Fingerprint Recognition Research Published

Approach	Technique	Info. on images	# of Classes	Comments
Jain et al. 1999 [6]	classification	1972 (28 rejected) training and 1965 (35 rejected) testing	4 or 5	No specific information on rejected images
Cappelli et al. 1999 [3]	classification	1204 pairs selected per occurrence of 5 classes	5	Compare continuous and exclusive classifications
Halici et al. 1996 [5]	classification	The first 500 pairs: 500 training and 500 testing	At most 15	Results depend on the number of classes and the size of search space
Kovacs-Vajna 2000[7]	verification	Manually rejected about 6%	N/A	No specific information on rejected images
Senior 2001 [11]	classification	First 1000 pairs training and second 1000 pairs testing	4	Shows test results for the second 1000 pairs only, which are correlated
Karu and Jain 1996 [12]	classification	2000 pairs	4 or 5	40 pixels along the borders of the direction image are removed
This paper	Indexing	2000 test images are completely processed without any handcrafting of the data	N/A	Rank ordered top N hypotheses are considered as a possible match to a query fingerprint

and identification is carried out during the online stage. During the offline stage, fingerprints in the database are processed one-by-one to extract minutiae [1] to construct model database. During the online stage, the query image is processed by the same procedure to extract minutiae. Indexing components are derived from the triplets of minutiae locations and used to map the points in the feature space to the points in the indexing space. The potential correspondences between the query image and images in the database are searched in a local area in the indexing space. An indexing score is computed based on the number of triangle correspondences and candidate hypotheses are generated. The top N ranked hypotheses are the result of our indexing algorithm.

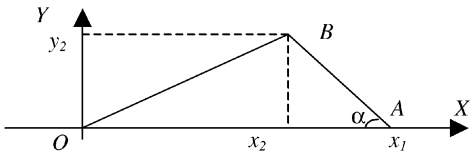

Fig. 1. Illustration of variables.

3.1 Analysis of Angle Changes Under Distortions

Without loss of generality, we assume that one vertex, O, of the triangle (see Fig. 1) is $(0, 0)$, and it does not change under distortions. Since distance is invariant under translation and rotation and relatively invariant under scale, and angles are defined in terms of the ratio of distance, it can be proven that angles are invariant under these transformations. However, because of uncertainty of minutiae locations, the location of each vertex changes independently in a small local area in a random manner. Suppose the locations of points A and B are $(x_1, 0)$ and (x_2, y_2), $x_1 > 0$, $y_2 > 0$, and $x_2 \in (-\infty, +\infty)$. We have $tan\alpha = y_2/(x_1 - x_2)$. Because of the uncertainty of minutiae locations, A and B move to $A'(x_1 + \Delta x_1, 0)$ and $B'(x_2 + \Delta x_2, y_2 + \Delta y_2)$, respectively, and α changes to $\alpha + \Delta\alpha$, then

$$tan\Delta\alpha = ((x_1 - x_2)\Delta y_2 - y_2(\Delta x_1 - \Delta x_2)) / ((x_1 - x_2)^2 + (x_1 - x_2)(\Delta x_1 - \Delta x_2) + y_2^2 + y_2\Delta y_2).$$

Suppose $| \Delta x_1 - \Delta x_2 | << | x_1 - x_2 |$, and $| \Delta y_2 | << | y_2 |$, and for small $\Delta\alpha, tan\Delta\alpha \approx \Delta\alpha$, we have

$$| \Delta\alpha | \leq | \Delta y_2 | / (2 | y_2 |) + | \Delta x_1 - \Delta x_2 | / (2 | x_1 - x_2 |).$$

TABLE 3
Expectation of the Percentage of Angle Changes Less than Various Thresholds

Angle's type	Angle change thresholds					
	$\pm 1^o$	$\pm 2^o$	$\pm 3^o$	$\pm 4^o$	$\pm 5^o$	$\pm 6^o$
α_{min}	51.6	93.2	98.5	99.6	99.9	100.0
α_{med}	56.6	87.3	94.5	97.3	98.7	99.4
α_{max}	1.0	67.7	87.3	94.2	97.2	98.7

That is, if the changes of minutiae locations are small enough, the change of the angle will be less than a certain small value. Furthermore, we can compute the expectation of $\mid \Delta\alpha \mid$. Let $f(x_1, x_2, y_2, \Delta x_1, \Delta x_2, \Delta y_2) = tan\Delta\alpha$. Suppose Δx_1, Δx_2, and Δy_2 are independent, and $-4 \leq \Delta x_i \leq 4$, $-4 \leq \Delta y_2 \leq 4$, $i = 1, 2$, and Δx_i and Δy_2 are all integers, we have

$$g(x_1, x_2, y_2) \approx \sum_{\Delta x_1 = -4}^{4} \sum_{\Delta x_2 = -4}^{4} \sum_{\Delta x_3 = -4}^{4} (\mid f(x_1, x_2, y_2, \Delta x_1, \Delta x_2, \Delta y_2) \times p(\Delta x_1) p(\Delta x_2) p(\Delta y_2) \mid .$$

Assuming $p(\Delta x_1)$, $p(\Delta x_2)$ and $p(\Delta y_2)$ are all discrete uniform distributions in $[-4, +4]$. Let $0 < x_1 < L$, $0 < y_2 < L$ and $\mid x_2 \mid < L$, where L is the maximum value (150 pixels in experiments) of these variables in the fingerprint. We compute $g(x_1, x_2, y_2)$ at each point (x_1, x_2, y_2). Table 3 shows the expectation of the percentage of angle changes that are less than various thresholds for the minimum, median and maximum angles in a triangle. We observe: 1) We should use $\alpha_{\min}$ and α_{med} as the indexing components to construct the model database; 2) $2^o - 4^o$ can tolerate most distortions of uncertainty and keep the size of the indexing space that need to be searched as small as possible. We also tried other distributions for $p(x_1)$, $p(x_2)$ and $p(y_2)$ and found similar results. Thus, *minimum angle and median angle in a triangle formed by the triplets of minutiae can be taken as components of the index to construct a model database for fingerprint identification.*

3.2 Triplet-Based Features for Indexing

The following features are derived from the triangle formed by each noncollinear triplets of minutiae to form index $H(\alpha_{min}, \alpha_{max}, \phi, \gamma, \eta, \lambda)$.

- **Angles α_{min} and α_{med}.** Suppose α_i are three angles in the triangle, $i = 1, 2, 3$. Let

$$\alpha_{max} = max\{\alpha_i\}, \alpha_{min} = min\{\alpha_i\}, \alpha_{med} = 180^o - \alpha_{max} - \alpha_{min},$$

  then the labels of the triplets in this triangle are such that if the minutia is the vertex of angle α_{max}, we label this point as P_1, if the minutia is the vertex of angle α_{min}, we label it as P_2, the last minutia is labeled as P_3 which is the vertex of angle α_{med}. Fig. 2 shows an example of this definition. We use α_{min} and α_{med} as two components of the indexing space. $0^o < \alpha_{min} \leq 60^o$ and $\alpha_{min} \leq \alpha_{med} < 90^o$.
- **Triangle Handedness ϕ.** Let $Z_i = x_i + jy_i$ be the complex number $(j = \sqrt{-1})$ corresponding to the location (x_i, y_i) of point $P_i, i = 1, 2, 3$. Define $Z_{21} = Z_2 - Z_1$, $Z_{32} = Z_3 - Z_2$, and $Z_{13} = Z_1 - Z_3$. Let triangle handedness $\phi = sign(Z_{21} \times Z_{32})$, where $sign(\bullet)$ is the sign function and $\times$ is the cross product. Since points P_1, P_2, and P_3 are noncollinear points, $\phi = 1$ or -1.
- **Triangle Type γ.** Each minutia is either an endpoint or a bifurcation, we define triangle type based on the types of minutiae that form the triangle. Let $\gamma = 4\gamma_1 + 2\gamma_2 + \gamma_3$, where γ_i is the feature type of point P_i, $i = 1, 2, 3$. If point P_i is an endpoint, $\gamma_i = 1$, else $\gamma_i = 0$. $0 \leq \gamma \leq 7$.
- **Triangle Direction η.** We search the minutia in the image from top to bottom and left to right, if the minutia is the start point of a ridge, we define the direction of the minutia $\nu = 1$, otherwise $\nu = 0$. Let $\eta = 4\nu_1 + 2\nu_2 + \nu_3$, where ν_i is ν value of point Pi, $i = 1, 2, 3$. $0 \leq \eta \leq 7$.
- **Maximum Side λ.** Let $\lambda = max\{L_i\}$, where $L_1 = \mid Z_{21} \mid$, $L_2 = \mid Z_{32} \mid$, and $L_3 = \mid Z_{13} \mid$.

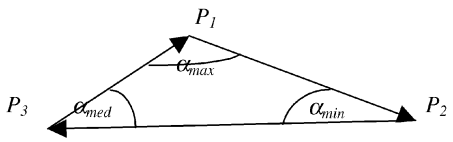

Fig. 2. Definition of feature points labels.

3.3 Geometric Constraints

They are used to reduce the number of false correspondences obtained from querying the lookup table by the index.

- **Relative local orientation at mid points.** Let points P_{21}, P_{32}, and P_{13} be the midpoint of line P_2P_1, P_3P_2, and P_1P_3, respectively, and point P_{123} be the centroid of the triangle $\Delta P_1P_2P_3$. Let $\varphi_{21} = \psi_{21} - \psi_{123}$, $\varphi_{32} = \psi_{32} - \psi_{123}$, and $\varphi_{13} = \psi_{13} - \psi_{123}$, where ψ_{21}, ψ_{32}, ψ_{13}, and ψ_{123} are the local orientations in the image at points P_{21}, P_{32}, P_{13}, and P_{123}, respectively. We assume that relative local orientations φ_{21}, φ_{32}, and φ_{13} will not change much in different impressions. So, $\mid \varphi - \varphi' \mid < \delta_m$, where φ and φ' are φ_{21}, φ_{32}, or φ_{13} in two different impressions.
- **Relative local orientation at vertices.** Let ψ_i be the local orientation of point P_i, and $\omega_i = \psi_i - \psi_{123}$, we have $\mid \omega - \omega' \mid < \delta_l$, where $i = 1, 2, 3$, and ω and ω' are ω_1, ω_2, or ω_3 in two different impressions of the same finger.
- **Relative translation**. Let $Z_c = (Z_1 + Z_2 + Z_3)/3$, where Z_i is defined in Section 3.2, we have $\mid Z - Z' \mid < \delta_t$, where Z and Z' are the Z_c in two different impressions of the same finger. $\mid Z - Z' \mid$ is the translation between the centroids of these two triangles.
- **Relative rotation**. Let $\theta_{21} = angle(Z_{21})$, $\theta_{32} = angle(Z_{32})$, and $\theta_{13} = angle(Z_{13})$, where Z_{21}, Z_{32}, and Z_{13} is defined in Section 3.2, and $angle(Z)$ is the phase angle of Z. Let $\mid \theta - \theta' \mid < \delta_r$, where θ and θ' are θ_{21}, θ_{32}, or θ_{13} in two different impressions of the same finger.

3.4 Indexing Score, Algorithms, and Analysis

Suppose

1. I is the query image and I_i are the images in the database, $i = 1, 2, \ldots N_d$, where N_d is the number of images in the database,
2. M and M_i are the sets of minutiae in I and I_i, respectively,
3. m is a minutia, and $m \in (M \cup M_i)$,
4. N_i is the number of matched triangles between I and I_i, $C_3^{n_i - 1} \leq N_i \leq C_3^{n_i}$, and n_i is an integer, which is the number of potential corresponding minutiae in each image, and
5. r is the number of triangles in I_i which include m. Then, we can compute the posterior probability

(1) For i = 1 to N, do 2 and 3
(2) Compute local orientation and extract minutiae locations in image I_i using feature extraction procedure.
(3) For each triplets in image I_i, compute α_{min}, α_{med}, ϕ, γ, η, *and* λ for the triangle formed by the triplets, and add this model together with the information required by the constraints for this model into the model database.

(a)

Suppose α_1 and α_2 are thresholds for α_{min} and α_{med} to deal with the changes in these angles.
(1) Compute local orientation and extract minutiae locations from the test image I.
(2) For each triplet in image I, do 3 and 4.
(3) Compute α_{min}, α_{med}, ϕ, γ, η, and λ for the triangle formed by the triplet.
(4) For $k_1 = -T_{\alpha 1}$ to $+ T_{\alpha 1}$ step 1, do
  For $k_2 = - T_{\alpha 2}$ to $+ T_{\alpha 2}$ step 1, do
    (4.1) Search the index space using $(\alpha_{min} + k_1)$, $(\alpha_{med} + k_2)$, ϕ, γ, η, and λ as the elements of index.
    (4.2) If the triangle satisfies the subsequent geometric constraints defined in Section 3.3, then take it as a successful correspondence of the triangle in the database.
  End loop for k_1
End loop for k_2
(5) Suppose there are $\sum_{i=1}^{N_d} M_i$ corresponding triangles, where M_i triangles belong to the same image I_i, $i = 1,2,\ldots N_d$, and N_d is the number of images in the database. Let $M_{max} = max\{ M_i \}$.
(6) If $M_{max} < T$, then reject the test image, where T is the threshold for rejecting a test image (see Section 3.4 for estimation of T), Otherwise do following steps,.
(7) Compute index score S_i based on M_i for I_i.
(8) Sort S_i in a descending order, output top N hypotheses.

(b)

Fig. 3. Algorithms for runtime identification (online stage). (a) Algorithm for constructing the model database (offline stage). (b) Algorithm for runtime indentification (online stage).

$PM_i = P\{I_i = I \mid m \in (M \cap M_i)\} = c \cdot r$, where c is a constant factor that makes PM_i to be the correct posterior probability.

We sort PM_i for each m, and find the n_i largest probabilities, suppose they are p_k, where $k = 1, 2, \ldots n_i$. We define the index score of image I_i as:

$$S_i = \sum_{k=1}^{n_i} p_k.$$

- **Algorithms.** Fig. 3 shows the algorithms used in our experiments.
- **Probability of false indexing.** Suppose:

1. S is the size of the index space,
2. f_k is the number of triangles in the model database for image I_k, and these triangles are uniformly distributed in the indexing space,
3. b is the search redundancy for each triangle in the query image,
4. v_k is the number of corresponding triangles between image I and I_k, and
5. f_t is the number of triangles for the query image [8].

Then, the value of v_k that is greater than a threshold T can be approximated by the Poisson distribution

$$p\{v_k > T\} \approx 1 - e^{-\xi} \sum_{i=0}^{T} (\xi^i / i!).$$

where $\xi = f_t \times p_1$, $p_1 \approx bp_0$, $p_0 = f_k/s$. In our approach, in a triangle if $\alpha_{min} < \delta_\alpha$ or $\tau < \delta_\tau$, where τ is the minimum side of the triangle, then we do not use this triangle to build the model. We use 0.5^o as the bin size for angles α_{min} and α_{med}, δ_λ for λ, and we search the indexing space with the uncertainty of $\pm 2^o$. Hence, $\xi \approx 15.885$. Fig. 4 shows the curve of $P\{v_k\} > T$ with respect to T. When $T = 25, P\{v_k\} > T = 0.0121$. That is, if there is no image in the database corresponding to the test image, the probability of finding 25 corresponding triangles between the test image and any of the images in the database is about 0.0121. We can use $T = 25$ as the threshold to reject a test image which has no corresponding image in the database. Note that, while the triangles are not uniformly distributed in the model database, since we apply geometric constraints, T can be less than 25.

4 Experiments

4.1 Database and Parameters

The data set 1 contains 400 pairs of images and 200 single images. These images are collected from 100 persons on the same day by a Sony fingerprint optical sensor (FIU-500-F01) with the resolution of 300 *DPI* (see Fig. 5a). The size of these images is 248×120 pixels. Each pair of images is different impression of the same finger, one is used to construct the model database, and the other one is used as the query image. The single image data set is used to test the rejection performance. We subjectively classify these images according to their quality into three classes: good, fair, and poor. Most images in the database are of fair (33.2 percent) or poor quality

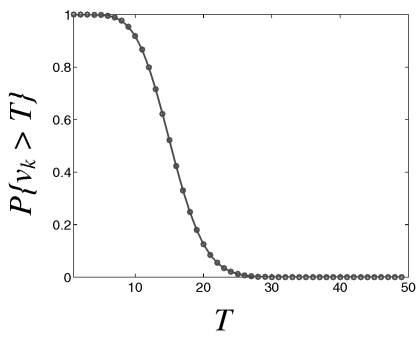

Fig. 4. $P\{v_k > T\}$ with respect to T.

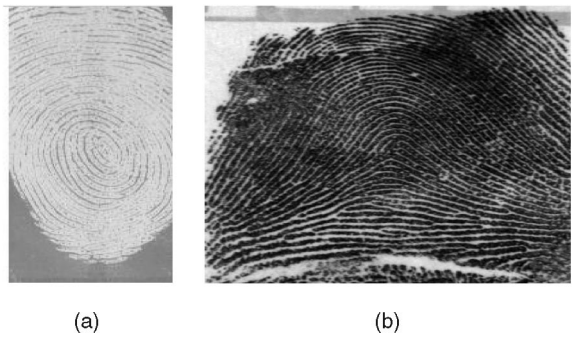

Fig. 5. Sample images: (a) data set 1 and (b) data set 2.

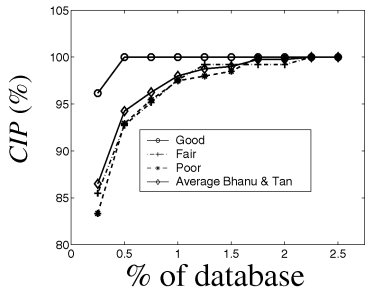

Fig. 6. *CIP* of data set 1.

(47.8 percent). The data set 2 is the NIST special database 4 (*NIST-4*) [9] that contains 2,000 pairs of images. Since these images are collected with an ink based method, a large number of *NIST-4* images are of much poorer quality. *NIST-4* images often contain other objects, such as characters and handwritten lines (see Fig. 5b). The size of these images is 480×512 pixels with the resolution of 500 *DPI*. Parameters δ_α, δ_τ, and δ_λ are different for the two data sets: for data set 1, $\delta_\alpha = 5^o$, $\delta_\tau = 20$ pixels, $\delta_\lambda = 10$ pixels, for data set 2, $\delta_\alpha = 10^o$, $\delta_\tau = 40$ pixels, $\delta_\lambda = 20$ pixels. All other parameters are the same for both data sets: $\delta_m = 30^o$, $\delta_l = 30^o, \delta_r = 30^o$, $\delta_t = 50$ pixels, $T_{\alpha 1} = 4^o$, $T_{\alpha 2} = 4^o$, and $T = 20$.

4.2 Performance Evaluation Measures for Indexing

False Positive Rate (*FPR*) and False Negative Rate (*FNR*) are used to evaluate the performance of a verification algorithm [10]. However, the goal of the indexing method in this paper is to narrow down the number of hypotheses which need to be considered for subsequent verification. The output of an indexing algorithm is the set of top N hypotheses. If the corresponding fingerprint is in the list of top N hypotheses, we should take the indexing result as a correct result. Hence, *FPR* and *FNR* are not suitable for evaluating the results of an indexing algorithm. We define Correct Index Power (*CIP*) and Correct Reject Power (*CRP*) as the performance evaluation measures for indexing: $CIP = (N_{ci}/N_d) \times 100\%$ and $CRP = (N_{cr}/N_s) \times 100\%$, where N_{ci} is the number of correctly indexed images, N_d is the number of images in the database, N_{cr} is the number of correctly rejected images, N_s is the number of the query images that don't have corresponding images in database.

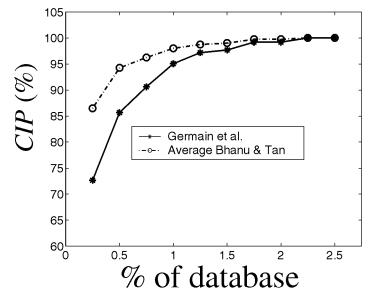

Fig. 7. Comparison of two approaches.

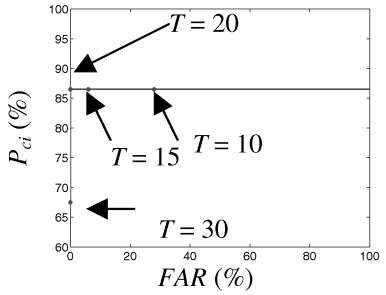

Fig. 8. ROC justifies $T = 20$.

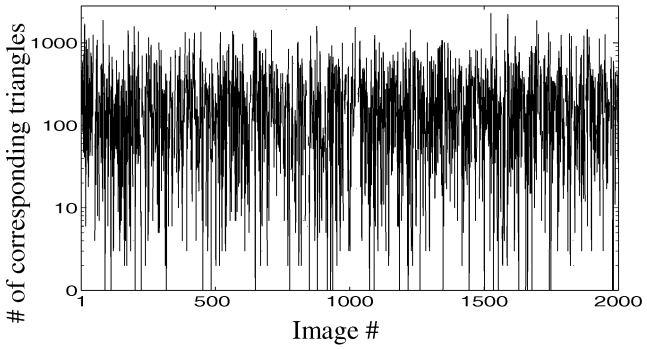

Fig. 9. Number of corresponding triangles of the 2,000 query images of data set 2.

4.3 Indexing Results for Data Set 1

Fig. 6 shows the *CIP* for each class of images and the entire data set 1 with respect to the length of the short list of hypotheses. The *CIP* of a single hypothesis for good quality images is 96.2 percent. As the quality of images become worse, the *CIP* decreases to 85.5 percent for fair and 83.3 percent for poor images. The average *CIP* of a single hypothesis for the entire database is 86.5 percent. The *CIP* of the top 2 hypotheses is 100.0 percent for good images, and for fair images and poor quality images, the *CIP* of the top five hypotheses are 99.2 percent and 98.0 percent, respectively. For the entire database of 400 images, the *CIP* of the top nine (2.3 percent of database) hypotheses is 100.0 percent. Fig. 7 shows that on data set 1 the performance of our approach is better than that of Germain et al.'s approach. We also evaluated the indexing performance of our algorithm for the 200 images, which are not in the database. Our indexing algorithm rejected these images $(CRP = 100\%)$. Thus, threshold T based on the analysis of

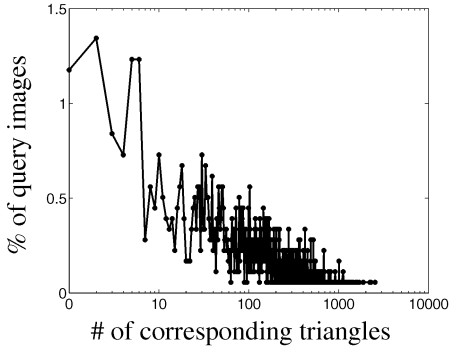

Fig. 10. Distribution of corresponding triangels among 2,000 query images of data set 2.

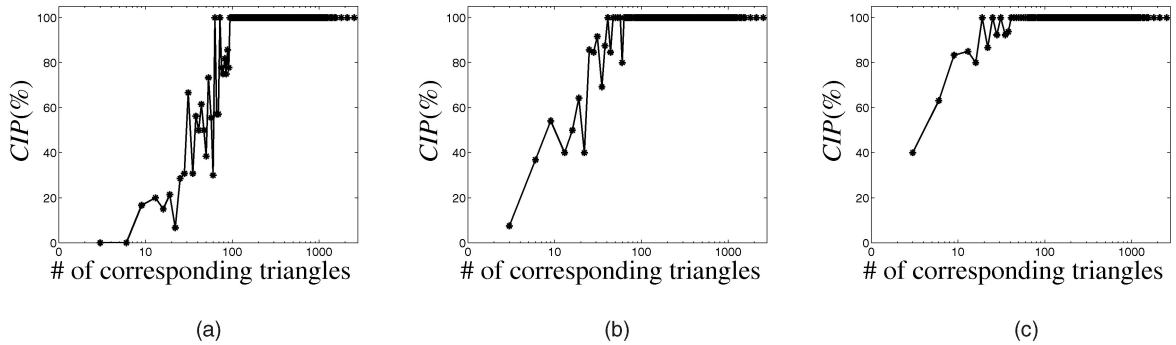

Fig. 11. CIP performance varies with the number of corresponding triangles (data set 2). (a) $\mathrm{T} = 1$, (b) $\mathrm{T} = 10$, and (c) $\mathrm{T} = 50$.

our approach works well. Furthmore, we use the hypothesis, which has the highest indexing score, as the result of identification to obtain the Receiver Operating characteristic Curve (*ROC*) shown in Fig. 8, where P_{ci} is the *CIP* for the top hypothesis and the False Alarm Rate $FAR = 100 - CRP$. When $T = 20$, the *FAR* is 0 and as T decreases, *FAR* will increase.

4.4 Indexing Results for Data Set 2

Fig. 9 shows the number of corresponding triangles for each query image of data set 2. Note that 32 images do not have any corresponding triangles. That is why *CIP* can not reach 100 percent as the number of hypotheses increases. Fig. 10 shows the distribution of the number of corresponding triangles among those 2,000 query images on a log scale. Because of bad quality, for some queries the number of corresponding triangles is quite small. Fig. 11 shows how *CIP* performance varies with the number of corresponding triangles for different threshold T. Approximately 10 good features lead to good indexing results.

- **Effect of constraints and computation time**. Fig. 12 shows the effect of geometric constraints in reducing the average percentage of hypotheses that need to be considered for indexing. We observe that four geometric constraints provide a reduction by a factor of 589.487, 6.869, 1.428, and 1.007, sequentially. On a SUN ULTRA2 workstation, without optimization, average time for correctly indexing or correctly rejecting a query is less than one second.
- **Extrapolation of indexing performance.** There exists no general theory in the computer vision and pattern recognition field to predict the performance of model-based indexing and matching algorithms under arbitrary transformations and arbitrary size of databases. Initial attempts have been made in [2], which takes into consideration of uncertainty in features, occlusion, clutter and similarity of object models. In the absence of a general theory, we perform extrapolation of the results obtained on *NIST-4* database to estimate the scalability of our approach. Let N, the number of hypotheses, be 10 percent of M, where M is the size of the database, but if $N > 100$, then let $N = 100$, so that the maximum number of hypotheses need to be considered is *100*. Fig. 13 shows the extrapolated performance of our approach on databases of different size, which uses a linear regression model. Fig. 14 shows the extrapolation with large M. As M increases, the performance will decrease and the 95 percent confidence interval of the performance will increase. However, these results indicate that a *CIP* of 50 percent could be achieved with a short list of 100 hypotheses, which would be only 0.33 percent of a 30,000-image database, which is really a good performance. This extrapolation from the results of 2,000 images to 30,000 needs to be taken with caution. It is dependent on the quality of input images and, as our analysis shows, *NIST-4* is a difficult database.
- **Comparison of approaches.** We have done a direct comparison with Germain et al.'s approach. We implemented Germain et al.'s approach and compared the performance of our indexing algorithm with it on *NIST-4* data set 2. Fig. 15 shows the comparisons of the two approaches on four subsets, first 100, 500, 1,000, and 2,000 fingerprints, of data set 2. Our approach has performed better than that of Germain et al.'s approach. When the entire data set 2 is used, although the *CIP* of Germain et al.'s approach increases from 53.0 percent to 67.0 percent, the *CIP* of our approach increases from 60.4 percent to 72.4 percent as the number of hypotheses increases from top 1 (0.05 percent of the database) to top 10 (0.5 percent of the database). Fig. 16 shows that the indexing performance increases as the percentage of the database size increases. When it is 10 percent, our approach is still better, the *CIP* of these two approaches are 85.5 percent and 83.7 percent, respectively.

A direct comparison with traditional fingerprint classification approaches can not be done for the following reasons: our approach for indexing is different from classification techniques. They are classifying each testing image into four or five classes, while we are generating the top N hypotheses for an input fingerprint query. The outputs of these two systems are different. If we take our approach

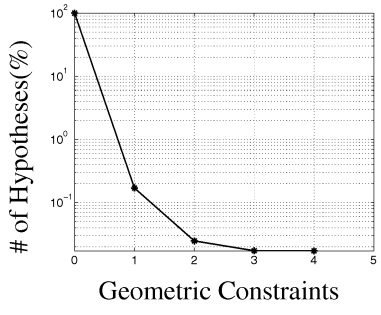

Fig. 12. Effect of constraints.

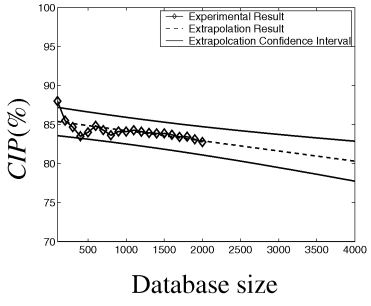

Fig. 13. Performance on *NIST*-4.

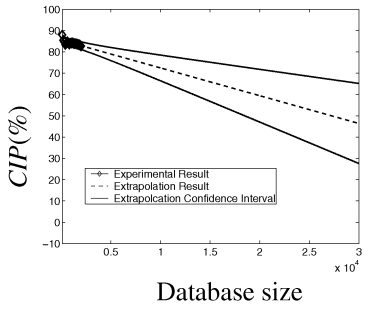

Fig. 14. Performance with large *M*.

and traditional classification approaches as a filtering step for data reduction before detailed verification, then it is possible to compare the two approaches indirectly. The results of our technique can be evaluated in term of the number of hypotheses that need to be considered for detailed verification. We do not use error/efficiency analysis since it has its own limitations as pointed out by Senior [11]. Fig. 15 and Fig. 16 show the percentage of the *NIST-4* database that needs to be examined in subsequent verification. Rather than reducing the computation for verification to about 1/3 of the database by a classification approach, our approach reduces the computation to about 10 percent of the database for the *CIP* to be 85.5 percent. So, on the *NIST-4* database, our approach is better than traditional classification approach. For a database of 30,000, for our approach, a *CIP* of 50 percent could be achieved with only 100 hypotheses (0.33 percent of the database). The performance of the traditional approach will be quite low, because the number of classes is limited (4 or 5) and quite likely there will be more than 10 percent misclassification. A thorough comparison of these two kinds of approaches (indexing and classification followed by verification) is the topic of future research. It is beyond the scope of this paper. Note that a low value for *CIP* is not a fatal flaw with our approach for large database where a low miss rate is required, because indexing can produce an ordered list of hypotheses of the entire database, which will, on average, be much more efficient for verification than a blind exhaustive search.

5 Conclusions

Our approach, based on triplets of minutiae, is promising for identifying fingerprints under translation, rotation, scale, shear, occlusion, and clutter. Experimental results show that it can greatly reduce the number of candidate hypotheses for further verification. In various comparisons with the prominent indexing approach developed by Germain et al., our approach has performed better. We have performed the analysis of the *entire NIST-4* database in a systematic manner and characterized indexing performance in terms of the number of corresponding triangles. This will allow the comparison of our results by others on the same publicly available

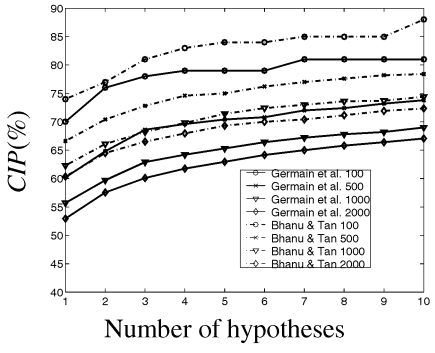

Fig. 15. Comparison of Germain et al.s and our approaches on *NIST*-4 data set.

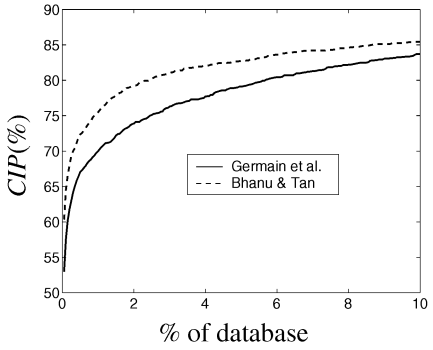

Fig. 16. Comparison of Germain et al.'s approach and our approach on *NIST*-4 data set.

database. Our approach can also be applied to each class after the fingerprints have been classified into R, L, A, T, and W classes to produce an ordered list of hypotheses for efficient verification.

Acknowledgments

This work was supported in part by grants from Sony, DiMI, and I/O Software.

References

[1] B. Bhanu and X. Tan, "Learned Templates for Feature Extraction in Fingerprint Images," *Proc. IEEE. Conf. Computer Vision and Pattern Recognition,* vol. 2, pp. 591-596, 2001.
[2] M. Boshra and B. Bhanu, "Predicting Performance of Object Recognition," *IEEE Trans. Pattern Analysis and Machine Intelligence,* vol. 22, no. 9, pp. 956-969, Sept. 2000.
[3] R. Cappelli, A. Lumini, D. Maio, and D. Maltoni, "Fingerprint Classification by Directional Image Partitioning," *IEEE Trans. Pattern Analysis and Machine Intelligence,* vol. 21, no. 5, pp. 402-421 May 1999.
[4] R.S. Germain, A. Califano, and S. Colville, "Fingerprint Matching Using Transformation Parameter Clustering," *IEEE Computational Science and Eng.,* vol. 4, no. 4, pp. 42-49, 1997.
[5] U. Halici and G. Ongun, "Fingerprint Classification through Self-Organizing Feature Maps Modified to Treat Uncertainties," *Proc. IEEE,* vol. 84, no. 10, pp. 1497-1512, 1996.
[6] A.K. Jain, S. Prabhakar, and L. Hong, "A Multichannel Approach to Fingerprint Classification," *IEEE Trans. Pattern Analysis and Machine Intelligence,* vol. 21, no. 4, pp. 348-359, Apr. 1999.
[7] Z.M. Kovacs-Vajna, "A Fingerprint Verification System Based on Triangular Matching and Dynamic Time Warping," *IEEE Trans. Pattern Analysis and Machine Intelligence,* vol. 22, no. 11, pp. 1266-1276, 2000.
[8] Y. Lamdan and H.J. Wolfson, "On the Error Analysis of 'Geometric Hashing'," *Proc. IEEE. Conf. Computer Vision and Pattern Recognition,* pp. 22-27, 1991.
[9] C.I. Watson and C.L. Wilson, "NIST Special Database 4, Fingerprint Database," U.S. Nat'l Inst. of Standards and Technology, 1992.
[10] J.L. Wayman, "Error Rate Equations for the General Biometric System," *IEEE Robotics & Automation Magazine,* vol. 6, no. 1, pp. 35-48, 1999.
[11] A. Senior, "A Combination Fingerprint Classifier," *IEEE Trans. Pattern Analysis and Machine Intelligence,* vol. 23, no. 10, pp. 1165-1174, Oct. 2001.
[12] K. Karu and A.K. Jain, "Fingerprint Classification," *Pattern Recognition,* vol. 29, no. 3, pp. 389-404, 1996.
[13] G. Jones and B. Bhanu, "Recognition of Articulated and Occluded Objects," *IEEE Trans. Pattern Analysis and Machine Intelligence,* vol. 21, no. 7, pp. 603-613, July 1999.
[14] V. Gaede and O. Gunther, "Multidimensional Access Methods," *ACM Computing Surveys,* vol. 30, no. 2, pp. 170-231, 1998.